Project	SEAMLESS No 101004032	**Deliverable**	D4.2
Dissemination	Internal/EC	**Type**	Report
Date	30th November 2022	**Version**	1.0

Deliverable 4.2

Recommendations for strongly coupled physical-biogeochemical data assimilation

Deliverable Contributors:	Name	Organisation	Role / Title
Deliverable Leader	Bertino L.	NERSC	Task 4.2 leader
Contributing Author(s)	Brasseur, P.	CNRS	Contributor
	Popov M.	UGA	Contributor
	Skakala J.	PML	Contributor
	Nerger L.	AWI	Contributor
	Wakamatsu T.	NERSC	Contributor
	Yumruktepe, C.	NERSC	Contributor
Reviewer(s)	Bertino, L.	NERSC	WP4 leader
	Ciavatta, S.	MOi	Advisory board

This project has received funding from the European Union's Horizon 2020 research and innovation programme under grant agreement No 101004032.

Project	SEAMLESS No 101004032	**Deliverable**	D4.2
Dissemination	Internal/EC	**Type**	Report
Date	30 November 2022	**Version**	1.0

Final review and approval	Skakala J.	PML	Project Coordinator

Document History:

Release	Date	Reason for Change	Status	Distribution
1.0	30-11-2022	Initial document, reviewed		Internal

To cite this document

Bertino. *et al.* (2022). D4.2 Recommendations for strongly coupled physical-biogeochemical data assimilation. Deliverable report of project H2020 SEAMLESS (grant 101004032.). doi 10.5281/zenodo.7432230

TABLE OF CONTENTS

Scope

The scope of this document is (i) to report on the developments of strongly coupled ensemble assimilation methods and assimilation experiments performed in WP4 (Task 4.2), and (ii) to provide methodological recommendations to perform strongly coupled physical-biogeochemical data assimilation in the 3D domains of the Monitoring and Forecasting Centers (MFC) of the Copernicus Marine Service (CMEMS).

Each partner in support of a particular MFC (AWI for BAL; NERSC for ARC, PML for NWS; UGA for GLO and IBI) implemented assimilation experiments in 1D or 3D setups as compliant as possible with the one used by the CMEMS systems in operation today, to facilitate the transfer of methods and results towards MFCs and to draw recommendations applicable to each MFC. This deliverable is building upon deliverable D3.2 (based on 1D experiments), deliverable D3.4 (based on 3D experiments), and D4.1 (on weakly coupled assimilation), and it addresses the prospects of coupled physical-biogeochemical data assimilation as deemed relevant for each MFC.

We note that the present version 1.0 of the Deliverable is not the final one, since it does not include the results from AWI for the assimilation system of the Baltic Sea. These results are delayed by a few months, due to current shortage of personnel, and will be integrated in the final version of this document, expected by month 30 of the project.

Introduction

The current operational bio-modelling systems *do not draw the maximum benefit* from assimilation of physical data, some even suffer deterioration of the biogeochemistry after assimilation of physical data. In view of the literature, the ensemble methods are the most adequate to tackle the problem of assimilating jointly ocean physical and biogeochemical data.

The overall objective of WP4 is to remove a blocking point for the mutual consistency of physical and BGC assimilation practices in CMEMS.

Our hypotheses are the following:

- Ensemble methods developed in WP3 can increase the reciprocal controllability of physical and biogeochemical states of the coupled models.
- Other methods can mitigate deteriorations.

This document is structured identically to D4.1 and as follow: In section 3 the choices for the experiment designs used in the different MFC domains are described. The results of the assimilation experiments obtained in the different MFC regions in Task 4.2 are reported in section 4. Ensemble diagnostics are described in terms of (i) observed state variables, (ii) non-observed state variables and (iii) relevant SEAMLESS indicators (leveraging from the conclusions of Tasks 3.2 and 3.3). In section 5, the results obtained for indicators are synthesized across MFCs with a focus on phenology, POC flux, primary production, grazing efficiency and PFTs (pH and O_2 being of lesser relevance following the

conclusions of Task 3.2 presented in the Deliverable D3.2). Finally in section 6, we provide guidelines for considering the implementation of strongly-coupled assimilation in the CMEMS MFCs.

Experimental Design Choices

In this section, the choices for the assimilation experiments in the MFCs are described. This builds on the assimilation methods developed and tested by the partners in Task 3.3, and the assimilation gaps that SEAMLESS aims to bridge with respect to the methods in operation today in the different centres. A schematic illustration of the transition from current to new ensemble-based assimilation methods as achieved by SEAMLESS for BGC monitoring and forecasting in the different MFCs is given in Table 3.1.

Partner	CMEMS MFC	1D Station	DA used in CMEMS	Target WP4 Method
NERSC	ARC	Station Mike	DEnKS	Ensemble
AWI	BAL	Arkona	LESTKF (fixed basis)	Ensemble
UGA	GLO / IBI (N. Atl.)	/	SEEK (fixed basis)	Ensemble
PML	NWS	L4	3DVAR	Hybrid Ens.-3DVAR

Table 3.1 Overview of model configurations and data assimilation methods used in this report.

3.1 Experimental design for the ARC MFC domain

GOTM 1D model.

The GOTM-FABM-ECOSMO 1D model (GOTM, hereafter), implemented in the SEAMLESS EAT prototype (see the Deliverables 2.1 and 2.2), is configured for the Argo float 6903554 in the Norwegian Sea (figure 4.1.1) for the strong coupled data assimilation experiment from March 2020 to October 2020. The spin-up run of GOTM is forced by the ERA5 hourly atmospheric forcing initialized with the world ocean atlas (WOA) climatology from 2011 to 2019 at the mean coordinate of the Argo float, (65.33N,1.75W) at first. Then, GOTM is forced by the ERA5 forcing extracted along trajectory from 2019 January 1st to 2020 December 31st to obtain a free run model state (figure 4.1.2). In the data assimilation experiment, the same free run configuration is used to generate the initial ensemble members with ensemble atmospheric forcing from 2019 January to 2020 March.

Observations.

The observed profile data of chlorophyll-a concentration, potential temperature and salinity are obtained from BGC Argo float data obtained from the Coriolis Data Centre and regridded to standard vertical depths and regular 10 days sampling interval (Figure 4.1.3). Sea surface observations of temperature (SST) and sea surface chlorophyll-a concentration (Chl-a) along the Argo float trajectory are obtained from the UK Met Office OSTIA SST dataset and the ESA OC-CCI dataset, respectively and interpolated to the Argo float sampling time and coordinate. All datasets are consistent with the latest CMEMS TAC products relative to Summer 2022.

The EAT data assimilation system.

The data assimilation (DA) system is the ensemble Kalman filter from the EAT DA package with. Ten days assimilation cycle intervals are applied. The initial ensemble with 80 ensemble members is generated by the GOTM ensemble runs with perturbations in wind forcing and ECOSMO model parameters from 2019 January to 2020 March. During each assimilation cycle, the atmospheric forcing and parameters perturbations are regenerated. The set of atmospheric variables to be perturbed is 10m zonal wind (u10), 10m meridional wind (v10) and the shortwave radiations. The set of parameters perturbed includes: maximum growth rate of large phytoplankton (muPl), maximum growth rate of small phytoplankton (muPs), large phytoplankton mortality rate (mPl), small phytoplankton mortality rate (mPs), large zooplankton mortality rate (mZl), small zooplankton mortality rate (mZs), detritus and opal sinking rate (sinkDet/sinkOPAL). 20% of the default value of each variable is given as standard error of perturbation. These choices are made following the current settings of CMEMS Arctic domain biogeochemical data assimilation system.

Experiment matrix.

Following Yu et al. (2018), the different DA setups used here with physical and biogeochemical coupled model are categorized as (table 3.1.1): 0-way, 1-way and 2-way categories. In Task 4.2, we conducted 2-way coupled DA experiments: Srf2Prf, Prf2Prf, TsrfChprf2Prf and TSprfChsrf2Prf, where TSprf stands for temperature and salinity profiles, Tsrf for surface temperature, Chprf for Chl-a profile, Chsrf for surface Chl-a and Nprf for nutrient profiles. Experiment Srf2Prf assimilates surface temperature and surface Chl-a observations and update the model states of temperature, salinity, Chl-a and nutrient (here after called "model state"). Experiment Prf2Prf assimilates temperature, salinity and Chl-a profiles and update the model state. Experiment TsrfChprf2Prf assimilates surface temperature and Chl-a profile and update the model state. Experiment TSprfChsrf2Prf assimilates temperature and salinity profiles and surface Chl-a and update the model state. Surface observations are obtained from the satellite-derived datasets and sub-surface observations (profiles) are obtained from the Argo float dataset.

Category	Experiment	Updated Fields (state)				Assimilated Observations				Note
		TSprf	Chprf	Pprf	Nprf	Tsrf	TSprf	Chsrf	Chprf	
0-way Weakly coupled	(Tsrf2TSprf)	√				√				
	(Tprf2TSprf)	√					√			
	Chsrf2BGCprf (control setting)		√	√	√			√		ARC MFC
	(Chprf2BGCprf)		√	√	√				√	
1-way	**Tsrf2Prf**	√	√	√	√	√				D4.2
	(TSprfPrf)	√	√	√	√		√			
	Chsrf2Prf	√	√	√	√			√		D4.2
	(Chprf2Prf)	√	√	√	√				√	
2-way	**Srf2Prf**	√	√	√	√	√		√		D4.2
	(Prf2Prf)	√	√	√	√		√		√	
	(TsrfChprf2Prf)	√	√	√	√	√			√	
	(TSprfChsrf2Prf)	√	√	√	√		√	√		

Table 3.1.1. Data assimilation setups. Blue hatched variables are from physical state and green hatched variables are from biogeochemical state. Acronyms are, T: temperature, TS: temperature and salinity, Ch: Chl-a, N: nutrient, srf: surface and prf: profile.

3.2 Experimental design for the BAL MFC domain

Assimilation method developed by AWI – to be completed by project month 30.

3.3 Experimental design for the GLO and IBI MFC domains

This section describes the design of the strongly coupled assimilation experiments implemented by **IGE/UGA** to assess how the 4D stochastic ensemble method developed in WP3 can be used to assimilate physical and biogeochemical data more consistently into the coupled NEMO-PISCES model, in the context of the GLO and IBI systems. The 4D space-time inverse approach developed in WP3 has been designed to avoid intermittent reinitializations of the coupled model, which is identified as a major source of issues in operational systems. This approach allows independent ("weakly coupled") or joint ("strongly coupled") assimilation of physical and biogeochemical data. As the assimilation system and experimental setup have been extensively described in D4.1, we focus here below on the specificities of the strongly coupled scheme.

The ***strongly coupled*** experiments carried out by IGE as part of Task 4.2d ***simultaneously*** combine the assimilation of CMEMS L3 along-track satellite altimetric data (SSH) and ocean colour (OC) data in the regional configuration intersecting GLO and IBI domains around the PAP station (48°50'N, 16°30'W), following WP3 developments. We use the same prior 40-member ensemble already generated during year 2019 (see D3.4), but we restrict its use during the period March 15th 2019 through June 15th 2019 (as in Task 4.1, see D4.1). During this 3-month period, the L3 CMEMS products include along-track data from 6 altimetric satellites (Sentinel-3A, Sentinel-3B, Jason-3, Cryosat-2, AltiKA, HY-2A) and daily ocean colour data at 4 km from 4 satellites (MODIS, VIIRS and Sentinel-3A/B sensors).

One-step observational update of the prior distribution by altimetric and surface ocean colour data. Altimetric observations from 4 satellites (Sentinel-3A/B, Jason-3, HY-2A) are assimilated jointly with OC L3 data during the period between March 15th and May 15th, using the LETKF analysis scheme implemented in 4D with all available observations included at once in the observation vector. The period from May 15th to June 15th is used to assess the predictive skill of the *probabilistic forecast*. This one-step update of the prior distribution mimics the strongly coupled assimilation concept as defined in SEAMLESS and differs from the weakly coupled scheme that requires two analyses steps. We use the same parameters for the localization scheme and observation error statistics as in Task 4.1.

The main focus in Task 4.2 is the assessment of the simultaneous update of the physical and BGC ensemble variables, and the comparison with the results of Task 4.1. In view of the nonlinear nature of the statistical model operator and the necessary approximations in the processing chain (anamorphic transformations, localization, ensemble inflation), the "weakly coupled" and the "strongly coupled" algorithms are likely to produce different results. This is investigated in Section 4.2.

3.4 Experimental design for the NWS MFC domain

The assimilation system is mostly identical to the used in Task 4.1 and described extensively in Deliverable 4.1. Here we focus the description on the most relevant differences of the system for strongly coupled assimilation. PML has run a 100-member ensemble experiment on the 1D L4 domain, using initial value and atmospheric perturbations. The experiment was run for the established 01/11/2014-31/10/2015 period. The relationship has been identified between the surface chlorophyll and SST variables, as shown in Fig.3.4.1. Fig.3.4.1 demonstrates that the Pearson correlation between SST and surface chlorophyll is substantially variable in time, but around the onset of the spring bloom period rapidly transits to R=-1 value. It is notable that this strong relationship between the variables

is probably influenced by the set of perturbations that are mostly physics driven (atmospheric forcing) and it is expected that if biogeochemical parameter perturbations were included the relationship would become much weaker.

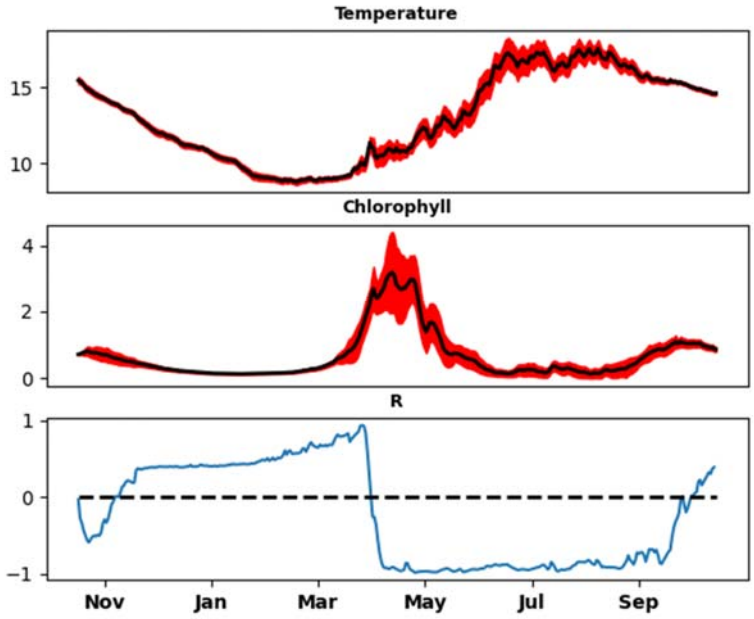

Fig.3.4.1: *The 1D 100-member ensemble simulation demonstrating the relationship (Pearson correlation, bottom panel) between the SST and surface chlorophyll at L4.*

The strong regime-change between the positive correlation and the strong negative correlation around April is interpreted as an effect of vertical mixing and light: in the period before the sudden transition in April (Fig.3.4.1) chlorophyll is not limited by nutrients, but is limited by light. The vertical mixing, which brings cold water to the surface, then easily carries phytoplankton into the deeper, darker waters, limiting its growth in the mixed layer. Simultaneously, stronger incoming surface radiance heats up the surface layer and supports the growth of chlorophyll. These two phenomena are likely to be jointly responsible for the positive correlation between SST and surface chlorophyll in the early Spring (Fig.3.4.1). The sudden transition to R=-1 shortly after the onset of the bloom, then corresponds to a new regime, when there is enough light availability, but the surface waters become more nutrient-depleted due to phytoplankton growth. The stronger the incoming light, heating up the ocean surface, the sooner and stronger the nutrients became depleted, and the more limitation they pose to chlorophyll in the period after the April transition. Simultaneously, the larger the vertical mixing bringing cold water to the surface, the more it drives also nutrient supply to the surface, supporting the growth of phytoplankton. Similarly to the pre-bloom period, we believe that the anti-correlation between surface chlorophyll and temperature is here a result of combined effect of incoming light and vertical mixing.

Only the perfect negative correlation that should dominate the period after the onset of the spring bloom was implemented into the balancing scheme on the 3D domain. The perfect negative correlation R=-1 between variables x and y implies the following relationship between their increments:

$$\Delta y = - (std(y)/std(x)) * \Delta x \qquad (1)$$

where "std" stands for the standard deviation. Because the SST increments are already delicately balanced with other physics variables, we decided to introduce the Eq.(1) only to the total chlorophyll increments, making it more consistent with the temperature. The balancing scheme therefore updated the total chlorophyll increments as

$$\Delta Chl\_iau = w1*\Delta Chl\_ibu - w2*[std(Chl)/std(SST)]*\Delta SST \ , \qquad (2)$$

where the index "_iau" means "increment after update" and "_ibu" means "increment before update". The weights w1, w2 were chosen to be in this case w1=w2=0.5. The std(Chl)/std(SST) had in the standardly used units (mg/m^3, C) at L4 a typical value of 0.15.

The system above was tested in a range of coupled assimilation runs in the 3D system of the NEW shelf. These runs copied what was done for the weakly coupled DA (see D4.1 report) in all aspects, except to the update to the balancing scheme: we assimilated satellite SST, EN4 T&S data and satellite OC total chlorophyll in the spring bloom period of 01/03-30/06/2018. To investigate the sensitivity of the strongly coupled assimilation to temperature updates, we included into the ensemble in one run temperature observation perturbations and in another we switched them off. Also, to prevent chlorophyll assuming unrealistic high values, we did a separate run where the strongly-coupled balancing scheme was switched off wherever the chlorophyll surface concentrations crossed a 10mg/m^3 threshold. Furthermore, since the perfect negative correlation between SST and surface chlorophyll (Fig.3.4.1) holds only for later part of the spring bloom period (May-June), we tried a separate strongly coupled simulation that started only on the 01/06/2018.

Assimilation experiments

This section reports on assimilation experiments of WP4.1 for the difference MFCs domains.

4.1 Assimilation results in the ARC MFC domain

Model bias.

Chl-a profile derived by the along Argo track free run (figure 4.1.2a) shows clear bias against observation (figure 4.1.3a). Over the upper layer ocean (100m and above) in the GOTM free run, the temperature is lower (colder) and the salinity is lower (fresher) compared to the Argo float observations. The difference becomes more significant once the surface mixed layer is developed in June and afterward. Under the mixed layer, there is clear sign of the Atlantic water characterised by warm and saline water in the Argo float data, but the signal is missing in the GOTM free run. This is mainly because the GOTM run along the Argo float trajectory is initialized by climatological temperature and salinity profiles which do not represent the Atlantic water realistically.

The onset of spring bloom both in the GOTM free run (figure 4.1.2a) and observation (figure 4.1.3a) is coming around mid-April, but the amplitude of the bloom is much stronger in the GOTM free run, as is often experienced in 3D models. There is a strong late-summer bloom in the observation, but the signal is completely missing in the GOTM free run. The deep mixed layer development and associated deepening of Chl-a layer can be observed in the Argo profile data, but the mixed layer depth development in the GOTM free run is underestimated and the associated Chl-a concentration is weaker.

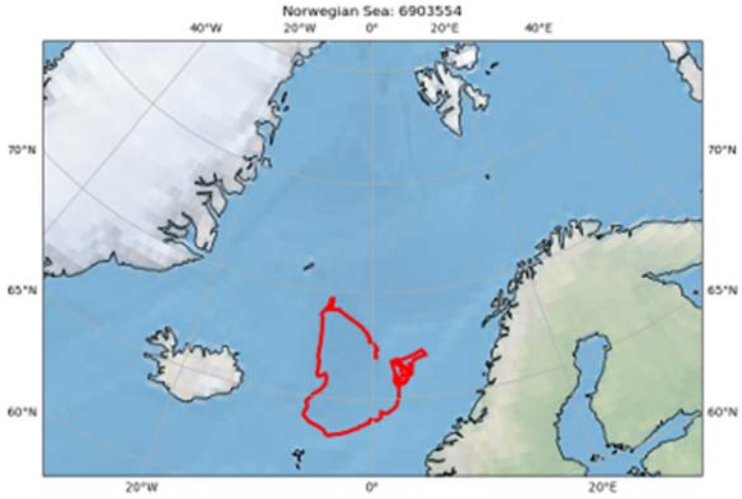

Figure 4.1.1. Trajectory of Argo float 6903554 in the Norwegian Sea.

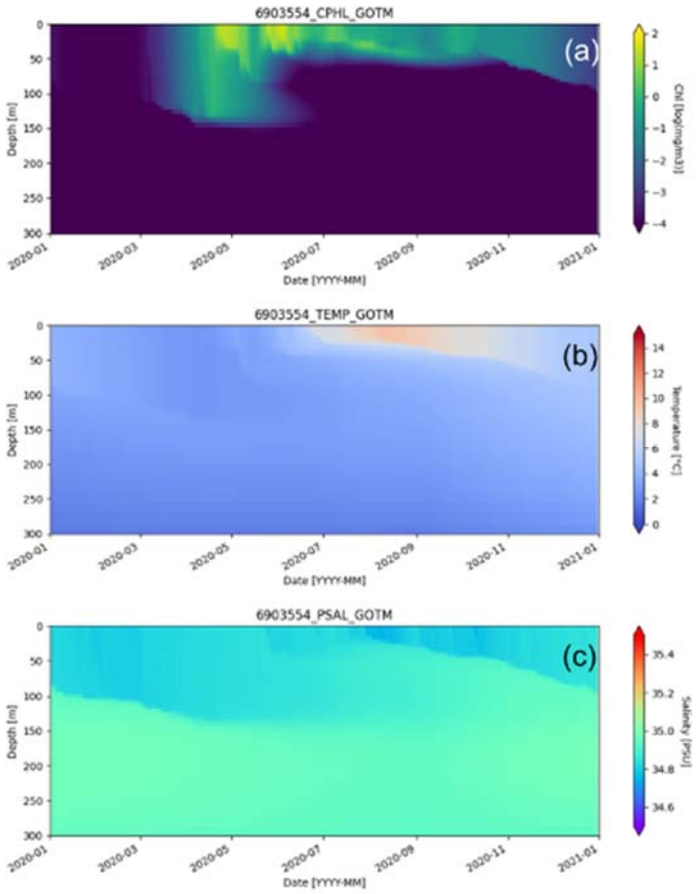

Figure 4.1.2. GOTM-FABM-ECOSMO 1D time series along the Argo float 6903554 in 2020. (a) Chlorophyll-a concentration [log(mg/m3)], (b) potential temperature [degree C] and (c) salinity [PSU].

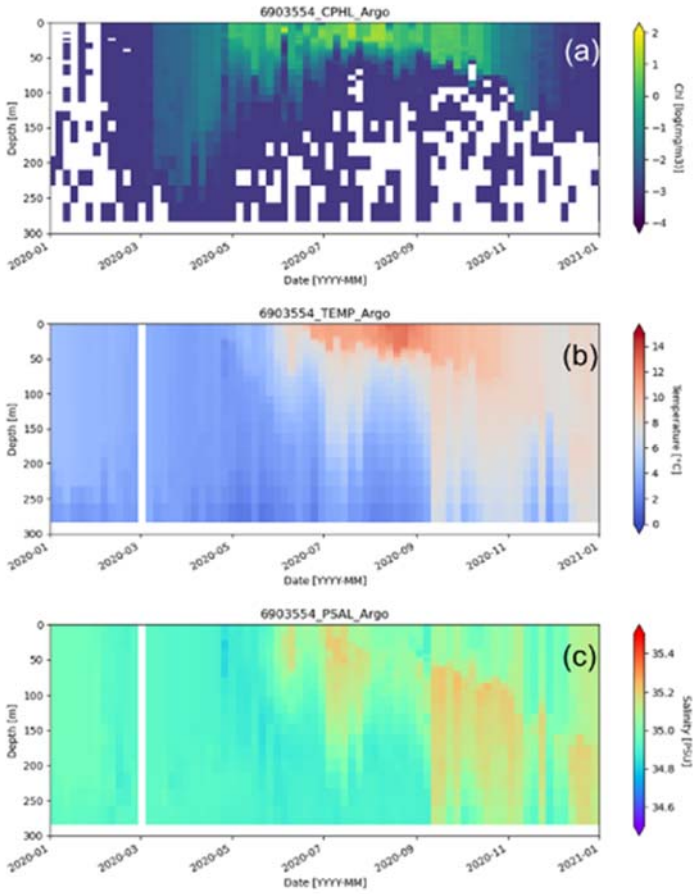

Figure 4.1.3. Observed 1D time series along the Argo float 6903554 in 2020. (a) Chlorophyll-a concentration [log(mg/m3)], (b) potential temperature [degree C] and (c) salinity [PSU].

True state and surface observation

Having a large model bias along the Argo float, we have decided to create a less challenging true state from a GOTM model run instead of the Argo profile data. The true state is generated from a GOTM single run using atmospheric forcing along the Argo float 6903554 in 2020, initialized from a climatological hydrographic profile at station M. The surface temperature and Chl-a are both sampled every 8 days from April 6th to October 6th 2020 and saved as surface observations for the data assimilation experiment. The standard deviation of all observations is set to 30% of the true value. Chl-a and nitrate profiles are depicted in Figure 4.1.4 (a,b).

Model ensembles

A model ensemble is generated by GOTM runs from 2019 January 1st to 2020 January 1st by giving 20% of perturbations to 10m wind and downward shortwave radiation at station M and 20% of perturbations to same ECOSMO model parameters as in the ARC MFC reanalysis after a model spinup running from 2011 January 1st to 2019 January 1st from the same initial condition used for generating the true state. Then a free model ensemble is conducted in 2020 with the same atmospheric and model parameter perturbations to serve as a lower benchmark for the data assimilation experiments.

Chl-a and nitrate profiles from the ensemble model free run are depicted in Figure 4.1.4(c,d). Compared to the true state, the timing of the spring bloom and associated timing of the declining nitrate is about 1 week too early (see also Figure 4.1.5a,b,d,e). The surface temperature is about 2 degrees higher than the true state and the deviation is especially large during June 2020 (Figure 4.1.5c). Such deviations are not uncommon in the Arctic MFC results.

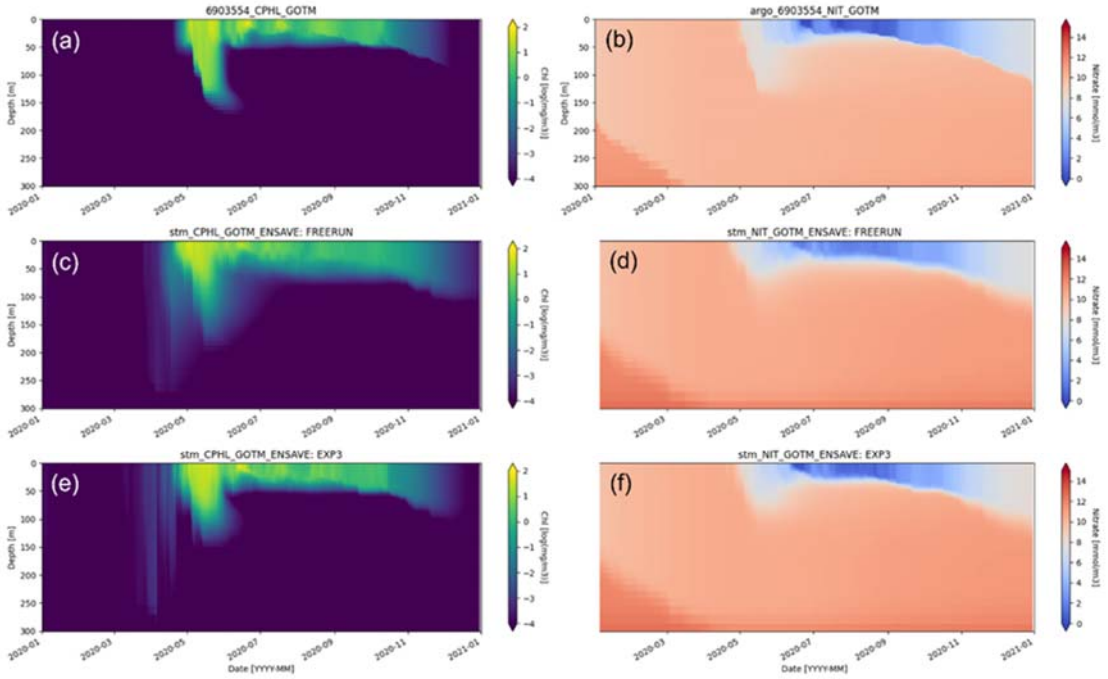

Figure 4.1.4. Chl-a profiles (left columns) and nitrate profiles (right columns) at station M in 2020. Top panels (a,b): True state, middle panels (c,d): Free run ensemble mean, Bottom panels (e,f): Data assimilation EXP3 analysis.

Summary of differences from the ARC MFC system

The **physical model** used in this deliverable is GOTM, discretized vertically in z-levels, while the ARC MFC is using the hybrid z-isopycnic coordinates from the HYCOM model. Although the mixed layer model is identical in both models, the definition of the state vector is different in the isopycnic domain as the BGC material is considered at a given density. The physical data assimilation does then shift the BGC material in the vertical and a post-processing procedure is then applied for mass conservation (Simon et al. 2015). This is not usually practiced in z-level models and is not applied here either. The latter step is formally a coupled assimilation feature from physical DA to BGC but was not considered in GOTM for the sake of simplicity. The ECOSMO II model is otherwise identical to the ARC MFC model.

The **data assimilation method** was the Ensemble Kalman Filter (EnKF) instead of the related one-lag smoother (EnKS). Since the impact of the smoothing step was less important than that of the filtering step (30% compared to 70%) and most of the methodological challenges are identical in both filter and smoother we have opted for the EnKF.

The **parameter estimation** feature was not utilised in the present experiments, although it has proven important in the ARC MFC reanalysis. This feature was not included yet in the EAT framework (planned for WP6) and was further motivation for using the EnKS instead of the EnKF.

The **Gaussian anamorphosis** (a logarithm) is applied both in the ARC MFC and the present experiments. Here all BGC variables are log-transformed, whereas the ARC MFC system only applies it to a few variables with documented lognormal probability distribution. Other variables – nutrients - are treated as Gaussian, only a limiter avoids negative concentrations after assimilation.

The above differences are reducing the analogy between the conducted experiment and the ARC MFC system but they make them more relevant for a broader community that does not use the above specificities.

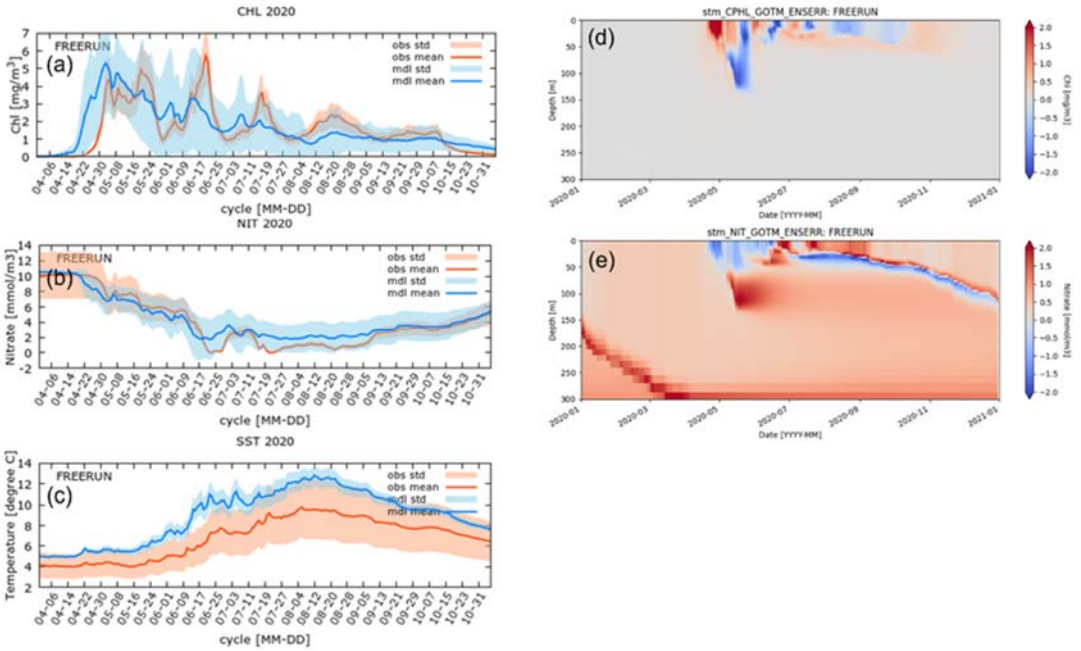

Figure 4.1.5. Model free run. Surface Chl-a, nitrate and temperature times series (left columns) and analysis error profiles (right column) from the free model run at station M. Top panels (a,d): total Chl-a, middle panels (b,e): nitrate and bottom panel (c): temperature. On the left columns, solid blue line is analysis mean, solid red line is true state and shades are respective standard deviations.

Impact of coupled data assimilation

Four data assimilation experiments, selected from the list of experiments in table 3.1.1, were conducted. Note that these are numbered from the most ambitious to the least ambitious:

- 2-way coupled data assimilation: EXP1 (Srf2Prf),
- 1-way coupled data assimilation: EXP2 (Tsrf2Prf), EXP3 (Chsrf2Prf)
- 0-way, weakly, coupled data assimilation: EXP4 (Chsrf2BGCprf).

EXP4 is the control experiment corresponding to uncoupled BGC data assimilation currently used for the ARC MFC BGC reanalysis system.

EXP1) Assimilation of surface Chl-a and surface temperature to update coupled model state (2-way).

Chl-a profiles (Figure 4.1.6a,d) show improvements of the Chl-a bloom timing and the following oscillations. The Root mean square error (RMSE) of the upper 30m Chl-a against the true state is improved to 0.847 mg/m3 starting from the free run where the RMSE is 0.957 (see Table 4.1.1). However, nitrate values started to increase unphysically after the assimilation cycle on June 17th 2020 (Figure 4.1.6b). The timing of the anomalous nitrate value development corresponds to a large correction of the surface temperature (Figure 4.1.6b), indicating there is a strong negative correlation between surface temperatures and nitrates in the model forecast ensemble and a transfer of the surface temperature bias to deep nitrates. After June 17th, the nitrates continue to keep high values throughout the entire assimilation period and the upper 30m RMSE against true states reaches as high as 18.3 mmol/m3. This type of transfer of biases has been punctually occurring in the ARC MFC reanalysis (between surface chlorophyll-a and deep nitrates) and their emulation in the 1-D prototype provides an opportunity to correct the problem.

EXP2) Assimilation of surface temperature to update coupled model state (1-way).

The impact of surface temperature assimilation is more significant in this 1-way coupled assimilation experiment, which is expected since the cost function has fewer terms here. Unfortunately after the model state update on the June 28th 2020 cycle, the ensemble forecast becomes numerically unstable and the EnKF assimilation cycles stop there (Figure 4.1.7a,b). An interesting observation is the improvement of the timing of the onset of the spring bloom even though the surface Chl-a is not assimilated (Figure 4.1.7a) before cycle May 16th 2020. This indicates that the correction of the surface stratification can regulate the timing of the Spring bloom onset. After May 16th 2020, the Chl-a analysis significantly overestimates the true state. This is again associated with the injection of nitrate to the model state after surface temperature assimilation, as previously seen in EXP1.

EXP3) Assimilation of surface Chl-a to update coupled model state (1-way).

The best RMSEs in both Chl-a and nitrate are observed in this experiment (Table 4.1.1). Compared to the 0-way assimilation experiment (EXP4), the most significant improvements can be found during the cycles between cycle August 12th 2020 and cycle September 5th 2020, when a peak of late-summer bloom is observed in the surface Chl-a (Figure 4.1.7c,e). During this period, surface Chl-s starts to decline immediately after its value is updated by Chl-a assimilation. The rate decline is however is weaker in EXP3 in which temperature and salinity profiles are updated coupled with BGC profiles. The reason is not clear and it requires further investigation.

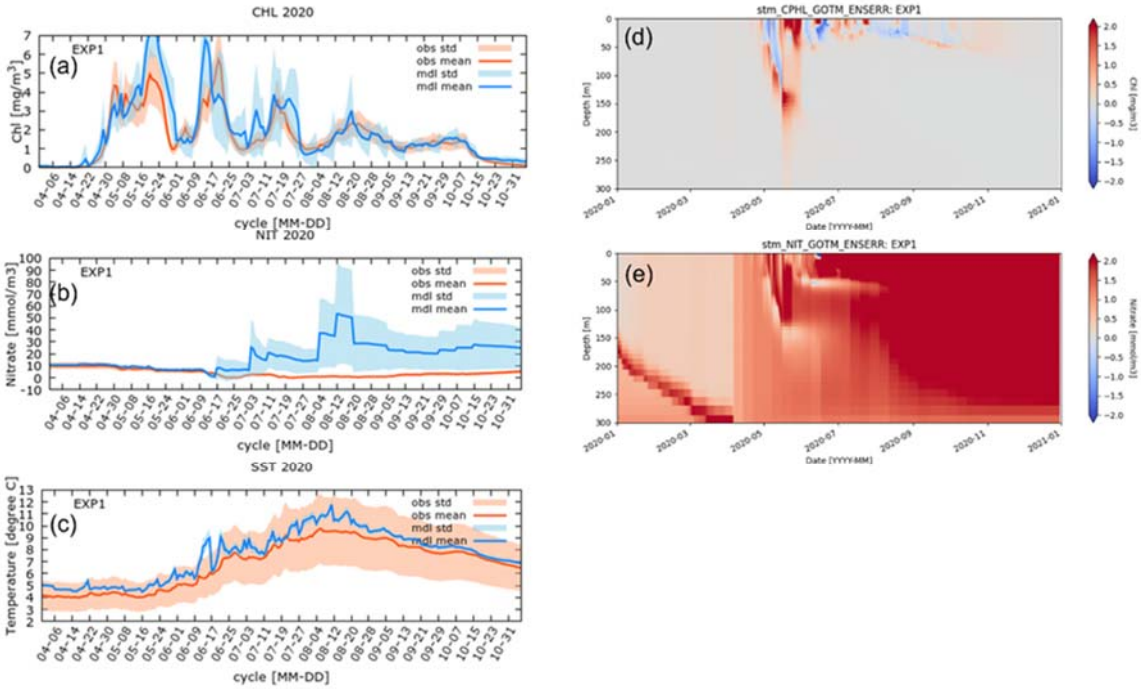

Figure 4.1.6. 2-way coupled data assimilation (EXP1). Surface Chl-a, nitrate and temperature times series (left columns) and analysis error profiles (right column) at station M. Top panels (a,d): total Chl-a, middle panels (b,e): nitrate and bottom panel (c): temperature. On the left columns, blue solid blue line is analysis mean, solid red line is true state and shades are respective standard deviation.

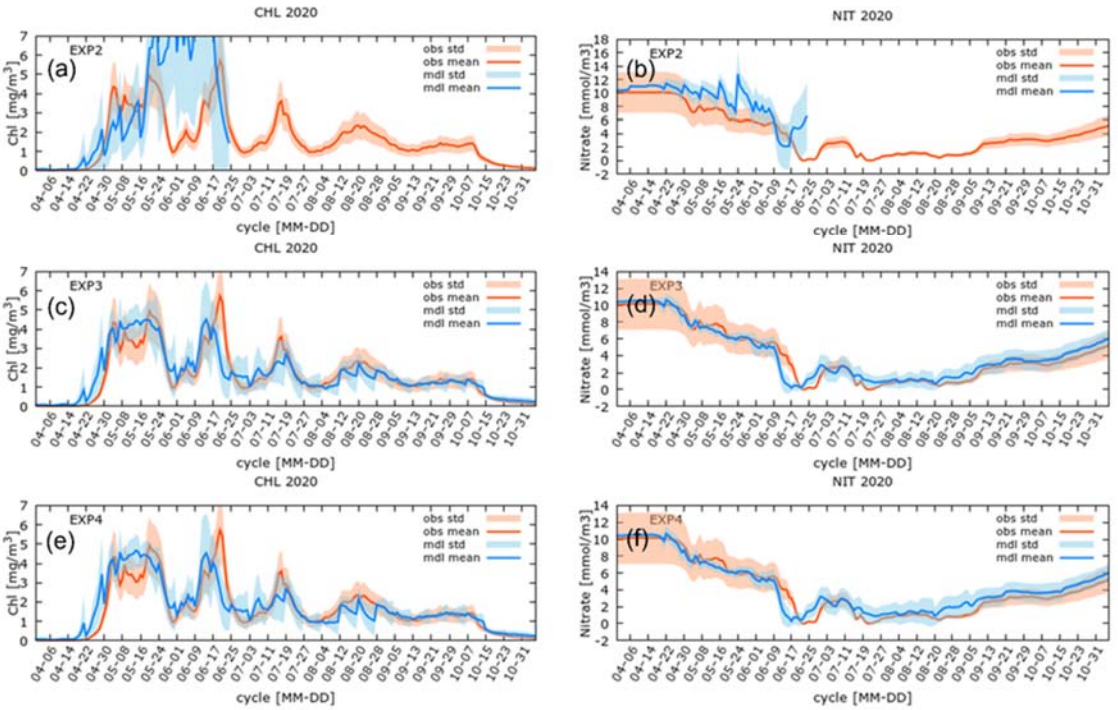

Figure 4.1.7. Surface Chl-a times series (left columns) surface nitrate time series (right columns) at station M. Top panels (a,b): EXP2, middle panels (c,d): EXP3 and bottom panel (e,f): EXP4. Solid blue line is analysis mean, solid red line is the true state and shades are respective standard deviation.

Diagnostics on non-observed variables

RMSEs of observed variable (Chl-a) and non-observed variables (nitrate and oxygen) in the upper 30m from data assimilation experiments and free run against true state are summarized in Table 4.1.1.

Experiment	Chl-a	Nitrate	Oxygen	Data Assimilation Settings	
				Observation	Model state
	RMSE [mg/m3]	RMSE [mmol/m3]	RMSE [mmol/m3]		
FREE	0.957	0.998	14.51	N/A	N/A
EXP1 (2-way)	0.849	18.30	5.335	SST, SCHL	T,S,BGC profiles
EXP2 (1-way)	N/A	N/A	N/A	SST	T,S,BGC profiles
EXP3 (1-way)	**0.635**	**0.718**	**14.17**	SCHL	T,S,BGC profiles
EXP4 (0-way)	0.675	0.805	14.58	SCHL	BGC profiles

Table. 4.1.1. Data assimilation (DA) settings and root mean square error (RMSE) of BGC variables (Chl-a, Nitrate and Oxygen) over the upper 30m depth against true state. Assimilated observations are sea surface temperature (SST) and sea surface Chl-a (SCHL). Model state updated by DA consists of temperature (T), salinity (S) and the selected BGC variables: Nitrate, Silicate, Phosphate, Phytoplankton biomass, Zooplankton biomass and Chl-a vertical profiles. EXP1 is the case of strongly coupled DA (2-way). EXP2 and EXP3 are weekly coupled DA (1-way). Note RMSE for EXP2 is not available due to instability in EnKF.

Diagnostics on derived quantities and indicators

Time series of derived variables, gross primary production (PP), particulate organic matter (POC), trophic efficiency (TE) and phytoplankton functional type (PFT) over the upper 200m depth from free run, data assimilation analyses EXP1, EXP2 and true state are plotted in figure 4.1.8. RMSEs of each derived variable against its true state are summarized in Table 4.1.2. Discussion on each derived variables can be found in section 5.2 (POC), 5.3 (PP), 5.4 (PFT) and 5.5 (TE).

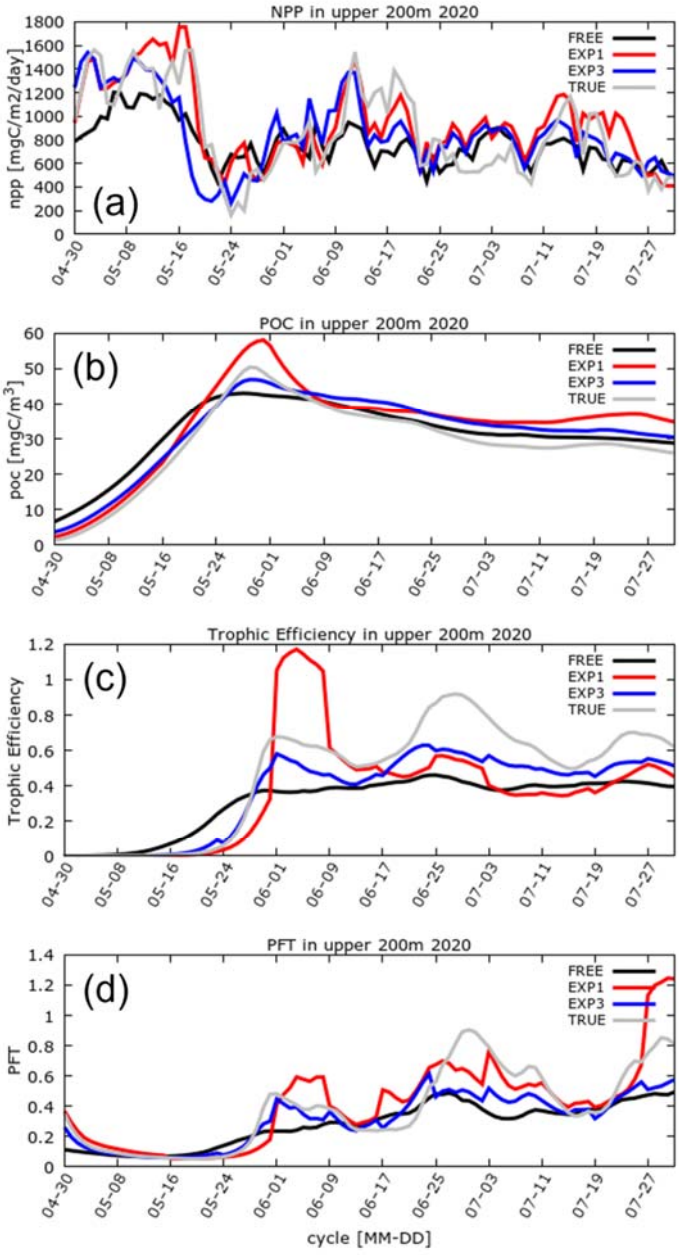

Figure 4.1.8. Time series of net primary production (NPP), particulate organic carbon (POC), trophic efficiency and phytoplankton functional type (PFT) over the upper 200 meter depth from ensemble model free run (FREE), 2-way (EXP1) and 1-way (EXP3) coupled data assimilation experiments and true state (TRUE).

Experiment					Data Assimilation Settings

	PP RMSE [mgC/m2/d]	POC RMSE [mgC/m3]	Trophic Efficiency RMSE	PFT RMSE	Observation	Model state
FREE	261.3	3.708	0.179	2.459	N/A	N/A
EXP1 (strongly 2-way coupled)	181.2	4.64	0.165	0.794	SST, SCHL	T,S,BGC profiles
EXP2 (1-way)	N/A	N/A	N/A	N/A	SST	T,S,BGC profiles
EXP3 (1-way)	**232.3**	2.924	**0.100**	**2.154**	SCHL	T,S,BGC profiles
EXP4 (weakly coupled)	246.0	**2.805**	**0.099**	**2.151**	SCHL	BGC profiles

Table. 4.1.2. Root mean square error (RMSE) of derived variables (PP, POC and Trophic Efficiency) over the upper 200m depth against true state.

4.2 Assimilation results in the BAL MFC domain

To be completed by project month 30.

4.3 Weakly coupled assimilation results in the GLO/IBI MFC domain

In this section we present the results obtained by **IGE/UGA** as part of Task 4.2d using the assimilation method described in Deliverable 3.4 and the strongly coupled experimental design described above.

Diagnostics on observed variables

The prior distribution is conditioned by all along-track altimeter and OC L3 data concatenated at once in the observation vector, resulting in the reduction of RMS statistics as shown in Figure 4.3.1. The posterior statistics are consistent with an expected error ~ 3cm in average (ensemble mean RMS error < 5 cm). The RMS difference with independent AltiKA measurements demonstrate the single update efficiency in terms of error reduction during the hindcast period; however, the benefit of the assimilated data disappears quite quickly after a few days of statistical forecasting. The statistics for the mean ensemble are similar to those of the weakly coupled experiment but the spread of RMS computed for each member is lower than in the weakly coupled experiment.

The corresponding ensemble mean of the reconstructed SSH is illustrated by Figure 4.3.2 for the situation of May 1st, showing a well-marked cyclonic eddy in the north-western corner of the domain. When compared to the equivalent map obtained with the weakly coupled scheme, the ensemble mean SSH pattern looks less noisy and more closely corroborated with the L4 SSH CMEMS product, based on the same altimeter tracks.

The SSH rank histograms shown in Figure 4.3.3 suggest that, during the hindcast period (centred on April 20th), the prior and posterior ensembles are quite consistent with independent (non-assimilated) altimeter data, but the posterior distribution has generated a significant number of outliers; this suggests that the ensemble has become under-dispersive, maybe as a result of the many observational data assimilated together (SSH + OC) in the one-step update. We can anticipate that the strongly coupled scheme is efficient in terms of SSH reconstruction, but slightly overconfident in terms of SSH uncertainty estimation. During the forecast period (centred on May 30th) the posterior is weakly impacted by the observations assimilated during the hindcast, while still increasing the number of outliers in the first rank.

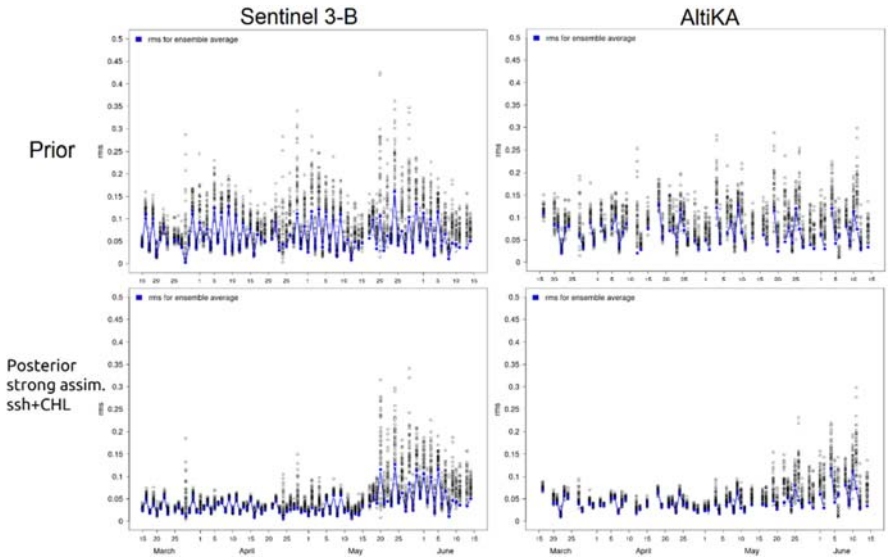

Figure 4.3.1: *RMS error statistics on SSH (in meter) computed daily during the 3-month experiment between ensemble members, ensemble mean (in blue) and assimilated Sentinel-3B (left) and non-assimilated AltiKA (right) altimeter data for the prior and the updated distribution using the strongly coupled scheme.*

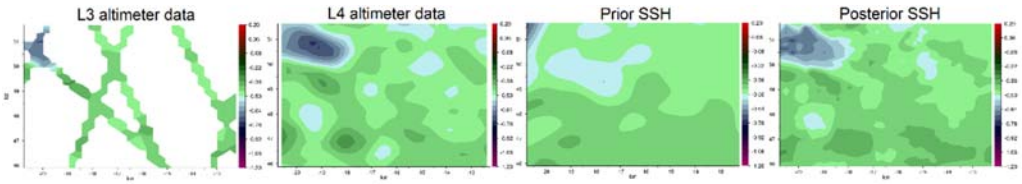

Figure 4.3.2: *SSH (in meter) in the PAP region for May 1st. From left to right: assimilated along-track CMEMS L3 SSH data; non-assimilated CMEMS L4 SSH data; ensemble mean of the prior distribution; ensemble mean of the posterior distribution in the strongly coupled scheme.*

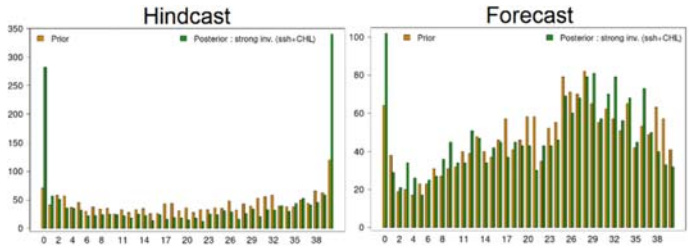

Figure 4.3.3: *Rank histograms for the PAP region calculated with the 2 non-assimilated satellite data sets (AltiKA, Cryosat-2) for 11-days periods in the hindcast (left) and forecast (right) periods. The brown bars represent the prior ensemble, the green bars represent the posterior ensemble after strongly-coupled observational update.*

Figure 4.3.4 shows the time series of chlorophyll concentration at PAP station in the prior ensemble and the posterior ensemble in the strongly coupled assimilation experiment. When comparing with the equivalent results in the weakly coupled experiment, we observe that the differences in the hindcast period are negligible. The only detectable change is the ensemble spread (standard deviation) near the end of the hindcast period, which is slightly larger in the strongly coupled experiment.

The spread of ensemble member RMS against assimilated OC data is slightly smaller in the strongly coupled experiment. In addition, we have computed the ratio of the posterior/prior ensemble variance used to quantify the reduction of uncertainty is now 0.205 in the PAP station area (instead of 0.321 in the weakly coupled case), i.e. a reduction of 54.7% (instead of 43.3% in the weakly coupled case) of the ensemble standard deviation, assuming 30% observation error variance. This confirms the tendency to provide lower uncertainty estimates of surface chlorophyll concentration in the strongly coupled assimilation case.

In the context of these experiments, **the strongly coupled experiment confirms the minor role of altimetry to control BGC processes**.

Figure 4.3.5 illustrates the reconstruction of surface chlorophyll patterns during the hindcast period. As in the weakly coupled case, the range of chlorophyll values in the posterior distribution agrees well with L3 or L4 products over the domain (this was not the case for the prior distribution). In addition, the consistency between observed and reconstructed spatial structures in cloud-free regions seems to be slightly improved when compared to the weakly coupled case. During the forecast period, the reconstruction (not shown here) indicates the same skill range as for the weakly coupled case.

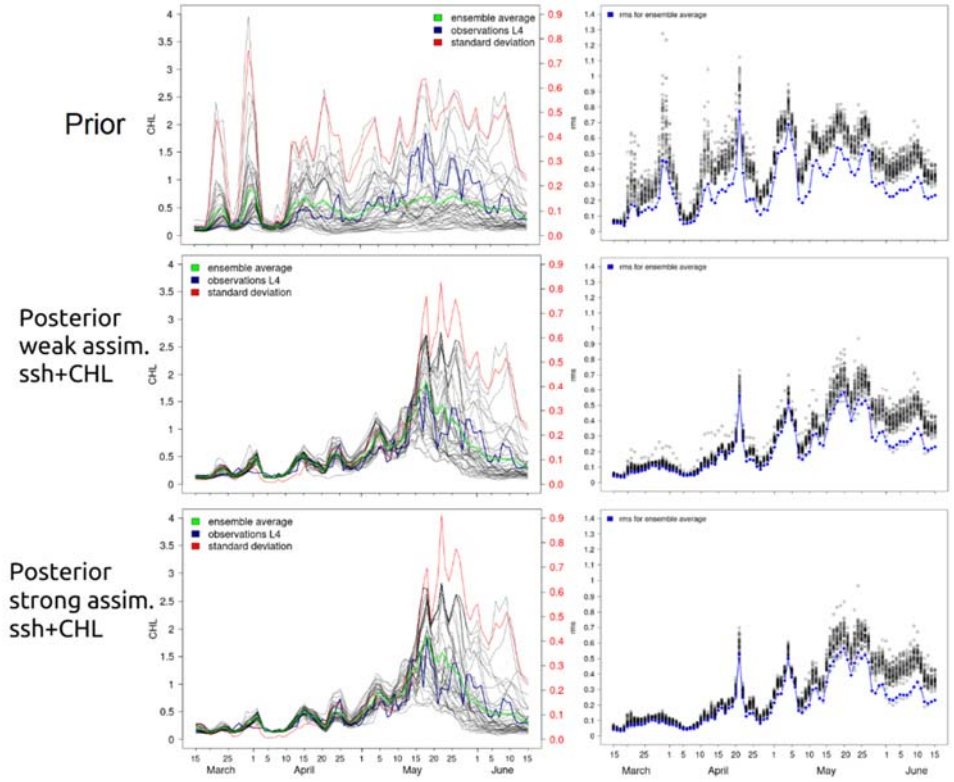

Figure 4.3.4: *Time series of the surface chlorophyll concentration (in mg/m3) at 16°30' W, 48°50'N (PAP station) for the prior (upper left), weakly coupled (centre left) and strongly coupled (lower left) posterior ensembles. The black curves show the 40-member ensemble; the green curve is the ensemble mean; the blue curve is the L4 CMEMS OC product collocated at PAP; the red curve is the standard deviation. Right panels: RMS error statistics on surface Chl computed daily between ensemble members, ensemble mean (in blue) and assimilated OC L3 data for the prior (upper right), updated distribution in the weakly coupled case (center right), and updated distribution in the strongly coupled case (lower right).*

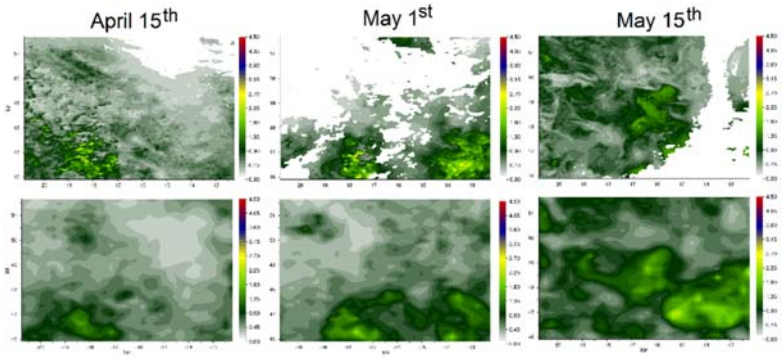

Figure 4.3.5: *Surface maps of chlorophyll concentration (in mg/m3) in the PAP station area (1100 km x 720 km centred on 16°30' W, 48°50'N) during the hindcast period (from April 15th to May 15th): CMEMS L3 product at 4km resolution (impacted by clouds) (upper row); posterior ensemble mean of the strongly coupled assimilation case (lower row).*

Diagnostics on "non-observed" variables

The assimilation impact on non-observed tracers such as nutrients and chlorophyll in the sub-surface euphotic zone has been diagnosed as in Task 4.1. This is illustrated by Figures 4.3.6, 5 days apart, for nutrient at PAP station, comparing results from the weakly coupled and strongly coupled assimilation. In the hindcast period (May 10th), both schemes reduce the spread of nutrient profiles by a factor of ~2, while the ensemble mean is nearly unchanged. After a 5-days forecast (May 20th), the assimilation impact is overall small. The impact at the end of the hindcast period (May 15th, with only past data being assimilated) is intermediate in terms of spread but the mean nitrate concentration is more than doubled. Further, it can be noted that the assimilation of physical data does not seem to introduce obvious inconsistencies in the BGC variables associated to, e.g. spurious vertical mixing.

The main difference between strongly coupled and weakly coupled cases is the posterior ensemble spread of nutrient profiles, which is systematically slightly larger in the strongly coupled case. This goes in the opposite direction as for observed variables in the strongly coupled case, with posterior distributions which seem to show under-dispersion.

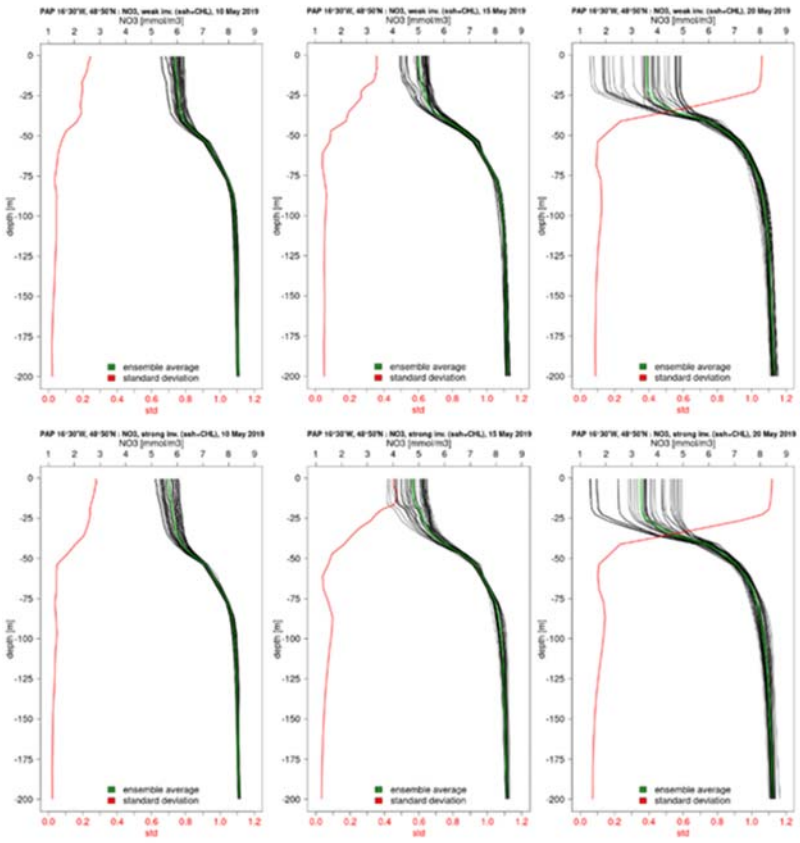

Fig. 4.3.6. *Weakly coupled (uppel row) and strongly coupled (lower row) posterior distributions of vertical NO3 profiles at 16°30'W, 48°50'N (PAP station) for May 10th, 15th and 20th. The black curves are the vertical profiles of the 40 ensemble members; the green curves are the ensemble mean; the red curves are the ensemble standard deviation.*

Diagnostics on derived quantities and indicators

The 3-month strongly coupled assimilation experiment is finally assessed in terms of impact on SEAMLESS indicators related to phytoplankton dynamics: vertical flux of particulate organic carbon (POC) at 100 meters, Trophic Efficiency in the upper 200 meters and vertically integrated Primary Production.

The statistics shown in Fig. 4.3.7 for the PAP station confirm that, during the spring period, the biogeochemical processes at depth are significantly influenced by the plankton dynamics in the upper layer when strongly constrained by surface data. As discussed earlier, the diagnostics calculated on the observed SSH and Chl variables suggest that this is mainly the result of assimilated ocean colour data, while altimetry has a very weak impact on the posterior distributions. The variance reduction is significant for the 3 indicators throughout the hindcast period and becomes negligible after a few days of forecasting. The ratio between posterior and prior ensemble variance for POC, Trophic Efficiency and Primary Production is slightly smaller than for the weakly coupled case.

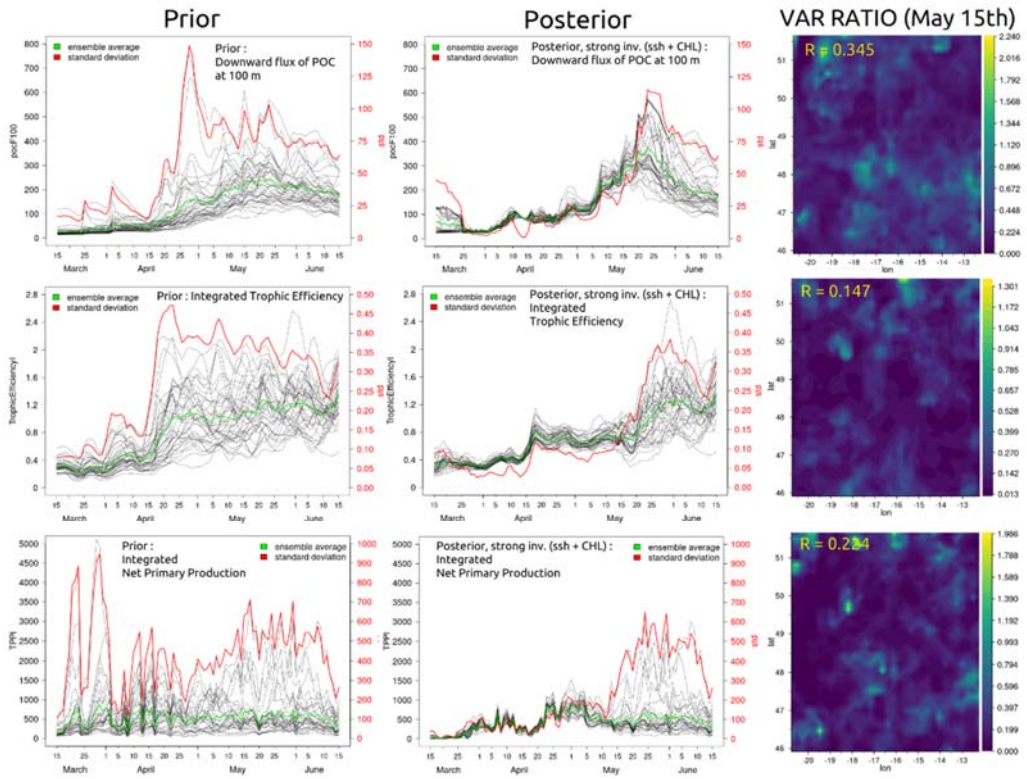

Fig. 4.3.7. *Time series of (i) (upper row) downward flux of the particulate organic carbon at 100-meter depth (in mg.C/m2/day); (ii) (middle row) Trophic Efficiency (ratio of vertically integrated values of total zooplankton and phytoplankton biomass between 0- and 200- meter depth) and (iii) (lower row) vertically integrated total Primary production (in mg.C/m2/day) at 16°30' W, 48°50'N (PAP station), for the prior (left panel) and posterior (central panel) ensembles of strongly coupled assimilation experiments. The black curves show the 40-member ensemble; the green curve is the ensemble mean; the red curve is the standard deviation. Right panel: ratio between posterior and prior ensemble variance in the region around PAP on May 15th (R is the average ratio over the area).*

Overall, the posterior ensemble mean of BGC variables and indicators are similar whether the data are assimilated in one step (strongly coupled) or two steps (weakly coupled), but the uncertainty estimates are smaller for the strongly coupled scheme. This is quantified in the PAP region on May 15th, as summarized in Table 4.3.1. We see that the differences between both schemes are less significant for non-observed quantities than for the observed BGC variable.

Indicator	Weakly coupled	Strongly coupled
Surface chlorophyll concentration	0,321	0,205
Particulate Organic Carbon flux	0,361	0,345
Trophic Efficiency	0,163	0,147
Net Primary Production	0,233	0,224

Table 4.3.1: *Uncertainty reduction in uncoupled, weakly coupled and strongly coupled experiments, estimated from the ratio between posterior and prior ensemble variance in the region around PAP on May 15th.*

Nevertheless, we would expect smaller uncertainty reductions for the unobserved indicators than for directly observed (and assimilated) surface chlorophyll concentration, regardless of the scheme used. It will therefore be relevant (i) to reconsider the uncertainty sources taken into account and their parameterization in an improved version of the NEMO-PISCES probabilistic model, and (ii) to extend the analysis to new areas of the North Atlantic to better understand how uncertainties propagate through the inversion chain. This will be the subject of new experiments planned in WP6.

4.4 Assimilation results in the NWS MFC domain

The physical-balancing equation successfully identified in the 1D system (see eq. 2 in Section 3.4) was applied with the 3D configuration of the model for the NW shelf.

All of the simulations performed for the NWS domain (with, or without observation perturbations, with applying 10mg/m*3 threshold for the balancing scheme and both for the full spring period and for the shorter period starting only in June) eventually led to unrealistically high concentrations of chlorophyll in parts of the domain that spread and substantially degraded the simulated biogeochemistry. The only difference between the output of the simulations was the time-scale on which the chlorophyll values became unrealistically high (e.g applying the 10mg/m*3 threshold could delay this degradation, but not overcome it). We believe that the substantial degradation to chlorophyll happened because the results obtained in the simplistic 1D configuration were not transferable straightforwardly to the complex 3D configuration in this case. One explanation for this might be the spatial variability in the SST – surface chlorophyl relationship, which would mean that 1D relationships are not representative of the full domain. Another possibility is that the 1D ensemble based on atmospheric perturbations was too simplistic to represent the SST – surface chlorophyll relationship. E.g including biogeochemical model parameter perturbations into the ensemble is expected to significantly lower the absolute value of correlation between the SST and surface chlorophyll. This would imply that linear relationship is not a good approximation to model the chlorophyll-temperature dependence and more complex (non-linear) relationships are needed. Capturing those and/or the spatial dependence of the surface chlorophyll-SST relationship, was however beyond the plan of SEAMLESS and needs to be explored in separate projects in the future.

5 Analysis of cost-benefits of strongly coupled DA

In this section, firstly we summarize the computational cost and benefits of performing strongly versus weakly coupled data assimilation in each MFC investigated in Task 4.2. Secondly, we synthetize the results obtained for the SEAMLESS indicators at each MFC with the exclusion of the NWS MFC, where the strongly coupled DA is not recommended with the system developed here (see Section 5.1.4). the results for the BAL system will be added at month 30 of the project.

5.1 Cost and benefits

5.1.1 ARC: Using either weakly or strongly coupled DA in TOPAZ with the EnKF would multiply the overall CPU costs by a factor 2.5 because of the integration of the ensemble of BGC models. This is a no-no for NRT operations, but acceptable for a reanalysis in delayed mode if the gains in quality are worth the costs. This discussion will be completed after the results are received.

5.1.2 BAL: To be completed at month 30 of the project

5.1.3 GLO/IBI: The CPU (and data storage) required to perform strongly coupled 4D inversions is half that of weakly coupled inversions. However, the cost for inversions is anyway negligible when compared to the prior ensemble production regardless of the scheme used. The numerical cost is therefore not a first-order criterion for choosing between weakly vs. strongly coupled 4D inversion strategy in an operational system.

5.1.4 NWS: At the current stage of the development, we do not recommend using the strongly coupled physical-biogeochemical DA system developed in SEAMLESS in the NWS domain. For now, the weakly coupled scheme should remain in use. We also recommend addressing the issues with strong coupling, with a more sophisticated scheme, where spatially varying (climatological) chlorophyll – SST relationships are used on the NWS domain. The ensembles developed in SEAMLESS can provide data to estimate the spatially varying (e.g., monthly) climatologies for important parameters, such as Pearson correlation coefficients. In addition to that, non-linear parametrizations of SST-surface chlorophyll relationship might be more useful than the linear models. In this case we highlight the potential use of machine learning (ML) models that can help to capture such relationships.

5.2 Surface Chlorophyll, phenology

In SEAMLESS, **the phytoplankton phenology** consists of three indicators (see deliverable D3.2): the value of the maximum of chlorophyll concentration in the layer 0-5m (mgChl m^{-3}), the depth of the maximum of chlorophyll during the summer period (m) and the timing of the bloom, i.e. the time of the year when the two maxima occur (day).

5.2.1 ARC: The best improvement in timing of spring bloom onset is found in the case of strongly coupled (2-way) data assimilation (Figure 4.1.6a). Considering that weakly coupled (1-way) data assimilation experiment with only sea surface temperature (SST) in observation shows improvement in the spring bloom onset timing (Figure 4.1.7a), it is speculated that SST assimilation has positive effect on estimating the early stage of the Phytoplankton phenology.

5.2.2 BAL: To be completed on Month 30

5.2.3 GLO/IBI: Phenology indicators can be retrieved from the reconstructed time series of the chlorophyll concentration in the productive layer. As for the weakly coupled scheme, the impact of the strongly coupled inversion on these indicators is significant, producing a much more intense spring bloom with a peak occurring ~ April 18th and a maximum value that coincides with the L4 data collocated at PAP station (Figure 4.3.4). However, the estimation of phenology indicators is not expected to be sensitive the chosen scheme.

5.3 POC flux

The **Particulate Organic Carbon (POC)** is considered here as the non-living carbon fraction of particulate organic matter, i.e. the detritus, and is computed as the average concentration of the 0-200m layer from the model output, or 0-bottom in shallower areas (Deliverable 3.2). Here we consider the POC flux, I.e. the sinking flux at a depth of 500m.

5.3.1 ARC: The time series of POC over the 200m depth is relatively insensitive to the different DA settings, considering the temporally integrated nature of the POC, (Figure 4.1.8b). Both strongly coupled and weakly coupled cases (EXP1, EXP3) show improvement in the timing of the peak of POC, compared to the model free run. This improvement is associated with the improvement in the phytoplankton phenology described in 5.2. The strongly coupled case overestimates the peak of POC compared to weakly coupled case, due to overestimated phytoplankton biomass. The latter, in turn, is due to the elevated surface nutrient caused by the assimilation of SST.

5.3.2 BAL: To be completed at month 30

5.3.3 GLO/IBI: In our 3D experiments, the POC flux is computed at the depth of 100 m, where some benefit can be expected from the improved chlorophyll estimates in the upper productive layer. The maximum POC flux increases in the strongly coupled assimilation, replicating the variability of the Chl concentration with a similar synchronicity. The impact of the strongly coupled assimilation is not significantly different from to the one observed in weakly coupled experiments.

5.4 Primary Production

The **primary production** is the synthesis of organic compounds from dissolved carbon dioxide through photosynthesis as source of energy. Primary production is computed as the vertical integral of the 0-200m layer. The unit is mmolC $m^{-2}d^{-1}$ (Deliverable D3.2)

5.4.1 ARC: The best improvement of primary production over the upper 200m depth, with respect the true state, is found in strongly coupled case (Figure 4.18a, Table 4.1.2). This improvement is mostly attributed to the improvements in the timing and period of the first peak of the spring bloom May (Figure 4.1.6a). After the first bloom peak, difference in strongly and weakly coupled data assimilation cases is not significant. This suggests correction of the surface stratification condition through SST assimilation has strong impact in estimating the spring bloom and its associated primary production.

5.4.2 BAL:

5.4.3 GLO/IBI: The impact of the strongly coupled inversion on Primary Production values during the spring bloom development cannot be considered as significant. The peak that occurs during the first weeks of April, though less intense than in the weakly coupled case, cannot be related to the major spring bloom. It could be an artefact of physical data assimilation. Further investigations are needed to better understand these results.

5.5 Phytoplankton functional types

The **Phytoplankton Functional Types** (PFT) indicator is defined as the ratio between large phytoplankton biomass and total phytoplankton biomass.

5.5.1 ARC: The first peak of PFT is seen during the early June in all experiments (Figure 4.1.8d). This indicates there is major shift in the phytoplankton composition from the 1st peak to the 2nd peak of the spring bloom in our model settings. Best improvement is obtained from strongly coupled case where only surface Chl-a is assimilated, while weakly coupled case underestimates the PFT.

5.5.2 BAL: To be completed by month 30.

5.5.3 GLO/IBI: This indicator was not evaluated in the GLO/IBI region.

5.6 Trophic efficiency

The **trophic efficiency** is the ratio of production at one trophic level to production at the next lower trophic level. See Table 2.1 of D3.2 for the definition for each of our BGC models.

5.6.1 ARC: During the peak in trophic efficiency (TE) in June (Figure 4.1.8c), the strongly coupled case largely overestimates TE against true state compared to the weakly coupled case. This degradation can be attributed to elevated nitrate concentration as a results of SST assimilation. PFT during the same period is overestimated against true state and zooplankton quicky increases its biomass. It requires further investigation to identify if this zooplankton over-reaction is due to direct impact of data assimilation or dynamical reaction for the increased phytoplankton biomass.

5.6.2 BAL:

5.6.3 GLO/IBI: Compared to the prior, the assimilation slightly reduces the trophic efficiency during the second half hindcast period (April 15th to May 15th). The ensemble spread is also reduced. The estimates during the forecast period (after May 15th) are not trustable. As for the weakly coupled case, further investigations (e.g., about the assimilation impact on zooplankton) are needed to understand these results.

The Table 5.1 summarises the main effects of the strongly coupled data assimilation on the SEAMLESS indicators in the different CMEMS domains.

Indicator	ARC	BAL	GLO/IBI
Phenology	degraded	TBC	minor impact
PP	changes	TBC	minor impact
POC flux	degraded	TBC	minor impact
PFT	improved	TBC	N/A
Trophic efficiency	changes	TBC	minor impact
pH	N/A	TBC	N/A
O_2	improved	TBC	N/A

Table 5.1. Summary of effects of the strongly coupled data assimilation in the CMEMS regions. The MED region is not part of the assessment on strongly coupled assimilation. The results are not reported for the NWS MFC, since the strongly coupled DA is not recommended in the NWS MFC with the system developed here (see Section 5.1.4).

6 Discussion and conclusions

6.1 ARC

In our twin data assimilation experiment settings, the actual errors arise from the following aspects:

- The surface forcing is causing a warm surface temperature bias
- Different initial conditions on 1st January 2020
- Biases arising from model non-linearity: the random model perturbations change the mean trajectory of the model and result in a bias, even if the perturbations have zero mean. Typically, the wind perturbations tend to deepen the mixed layer rather than making it shallower, on average.

The errors applied to the model (Section above) were only partially accounting for the actual errors: for example, the timing of the bloom was varying between members of the ensemble free run, but the truth was lying on the outskirts of the one-standard-deviation envelope.

We found that surface temperature assimilation significantly degrades the EnKF analysis in both strongly (2-way) and weakly (1-way) coupled cases. Since our model has a positive bias in its surface temperature against the true state, the anomalous elevation of nitrate value after temperature assimilation indicates there exists a strong negative correlation between temperature and nitrate ensembles within the mixed layer. The best result is obtained in the case (EXP3) of only assimilating surface Chl-a while updating coupled model state. These results were not those encountered by Yu et

al. (2018) obtained in a different idealized setup (a 3D channel experiment), which recommended the two-way coupled DA setup. In order to draw more general conclusions on the optimal choice of the coupled data assimilation settings, further investigation in the structure of forecast ensemble covariance of the coupled model state is warranted. For example, the present results were obtained with stronger biases than those in Yu et al. (2018) and may therefore lead to more conservative recommendations. One positive and Yu-et-al-consistent aspect from the above experiments is that the assimilation of surface Chlorophyll has shown advantageous to update the physics even though the observation errors were strong (30%) and the ECOSMO model had intrinsic uncertainties, which goes against the a-priori conception that ocean BGC observations and models are too uncertain to help updating the physics. The latter should be further tested with real BGC data.

The first perspective is to expand the sources of model errors based on the sensitivity analysis done in WP3. Having more independent sources of random noise can dissociate the spurious multivariate covariances. This part is the most interpretable as model errors can then be targeted as areas of improvement of the BGC model. Returning to the ensemble results in WP3 and scrutinizing the relationship between surface variables and deep nitrates in different ensemble setups should provide a clear way forward.

Another potential area of improvement is the fine-tuning of the anamorphosis function of BGC variables, which was a logarithm for all of them, although nutrients may be more normal than lognormal distributed.

Lastly, the brute-force approach to limit the effect of spurious covariances at depths is to apply vertical localisation of the assimilation so that the observations at the surface only have an effect within the mixed layer (Wang et al. 2022, in press).

6.2 BAL

To be added at month 30

6.3 GLO/IBI

The strongly coupled data assimilation, when using a 4-dimensional Monte-Carlo ensemble smoother assimilating real satellite observations, only shows moderate gains in the considered North Atlantic region without leading to degradations. Although this is encouraging in itself, the impact of assimilating the altimetry data on the biogeochemical variables was minor and probably unconvincing for the GLO MFC operations.

The recommendation is to consider longer assimilation windows in the GLO and IBI BGC assimilation systems, which would allow extended functionalities, like estimation of model parameters.

6.4 NWS.

At the current stage of development of the modelling systems, the strongly coupled data assimilation is not advised for the NWS MFC. Further future developments and testing of the system are recommended.

6.5 Overall conclusion

The coupled data assimilation experiments in Task 4.2 have taken some ambitious choices (assimilation of real measurements, advanced data assimilation methods, and a recently developed data assimilation software in EAT) in a 6-months period that did not leave much room for troubleshooting or for unavailability of personnel.

The scientific problems encountered were the following:

- Unrealistic high values of tracers (leading at times to filter divergence) were encountered in the NWS and ARC system with frequent data assimilation updates, although not in the GLO/IBI system. These problems are related to the transfer of biases from observed to non-observed variables in the ensemble covariances. They can be counteracted in the future
- At the other end of the scale, the lack of impact of the physical model on the biogeochemical model from the GLO/IBI experiment did not reproduce the problems encountered by the GLO/IBI MFC operations. The long data assimilation window does limit the unphysical effects of the linear updates.

A reasonable compromise should be obtained with intermediate length of the data assimilation window, taking advantage of the possibility for asynchronous assimilation in ensemble data assimilation.

We note that this section will be revised after the delayed inclusion of AWI's section on the Baltic MFC at month 30.

References

Berline L., Brankart J.M., Brasseur P., Ourmières Y. and Verron J., 2006: Improving the dynamics of a coupled physical-biogeochemical model of the North Atlantic basin through data assimilation: impact on biological tracers, J. Mar. Syst., 64, 153-172, https://doi:10.1016/j.marsys.2006.03.007.

Deliverable 3.2 - Ciavatta, S., Lazzari, P., Alvarez, E., Bruggeman, J., Capet, A., Cossarini, G., Daryabor, F., Nerger, L., Skakala, J., Teruzzi, A., Wakamatsu, T., Yumruktepe, C. (2022). D3.2 Observability of the target indicators and parameter sensitivity in the 1D CMEMS sites. Deliverable report of project H2020 SEAMLESS (grant 101004032), doi: 10.5281/zenodo.6580236

Gasparin F., Cravatte S., Greiner E., Perruche C., Hamon M., Van Gennip S. and Lellouche J.-M. (2021). Excessive productivity and heat content in tropical Pacific analyses: Disentangling the effects of in situ and altimetry assimilation, Ocean Modelling, 160, https://doi.org/10.1016/j.ocemod.2021.101768.

Pham, D.T., Verron, J., Roubaud, M.C., 1998. A singular evolutive extended Kalman filter for data assimilation in oceanography. Journal of Marine Systems 16, 323–340. https://doi.org/10.1016/S0924-7963(97)00109-7

Simon, E., Samuelsen, A., Bertino, L., & Mouysset, S. (2015). Experiences in multiyear combined state-parameter estimation with an ecosystem model of the North Atlantic and Arctic Oceans using the Ensemble Kalman Filter. *Journal of Marine Systems*, *152*, 1–17. https://doi.org/10.1016/j.jmarsys.2015.07.004

Wang, Y., Counillon, F., Barthélémy, S., and A. Barth (2022). Benefit of vertical localisation for sea surface temperature assimilation in isopycnal coordinate model. *Front. Clim. Sec. Predictions and Projections*. In press. doi: 10.3389/fclim.2022.918572

Yu, L., Fennel, K., Bertino, L., Gharamti, M. El and Thompson, K. R.: Insights on multivariate updates of physical and biogeochemical ocean variables using an Ensemble Kalman Filter and an idealized model of upwelling, Ocean Model., 126, 13–28, doi:10.1016/j.ocemod.2018.04.005, 2018.